Review

Application of Through Glass Via (TGV) Technology for Sensors Manufacturing and Packaging

Chen Yu , Shaocheng Wu , Yi Zhong , Rongbin Xu , Tian Yu , Jin Zhao , Daquan Yu *

Posted Date: 1 December 2023

doi: 10.20944/preprints202312.0064.v1

Keywords: Through glass via; MEMS sensors; Sensor manufacturing; Sensor packaging

Review

Application of Through Glass Via (TGV) Technology for Sensors Manufacturing and Packaging

Chen Yu [1], Shaocheng Wu [2], Yi Zhong [3], Rongbin Xu [4], Tian Yu [5], Jin Zhao [6] and Daquan Yu [2,*]

[1] Xiamen University; 36120211150419@stu.xmu.edu.cn
[2] Xiamen University; 36120211150391@stu.xmu.edu.cn
[3] Xiamen University; zhongyi@xmu.edu.cn
[4] Xiamen University; xurongbin@xmu.edu.cn
[5] Xiamen University; 36120200155810@stu.xmu.edu.cn
[6] Beijing University of Technology; zhaojin@emails.bjut.edu.cn
* Correspondence: yudaquan@xmu.edu.cn

Abstract: Glass has emerged as a highly versatile substrate for various sensor and MEMS packaging applications, including electromechanical, thermal, optical, biomedical, and RF devices, due to its exceptional properties such as high geometrical tolerances, outstanding heat and chemical resistance, excellent high-frequency electrical properties, and the ability to be hermetically sealed. In these applications, Through-Glass-Via (TGV) plays a vital role in manufacturing and packaging by creating electrical interconnections through glass substrates. This paper provides a comprehensive summary of the research progress in TGV fabrication along with their integrations, including through-via formation and metallization. The paper also reviews the significant qualification and reliability achievements obtained by the scientific community for TGV. Additionally, the paper summarizes the application of TGV technology in various sensors.

Keywords: Through Glass Via; MEMS sensors; Sensor manufacturing; Sensor packaging

1. Introduction

Due to the progress of 5G, smart cars, medical gadgets and other industries, electronic products are designed to be more portable and convenient. Much research has been invested in the fabrication, integration, and packaging of sensors, aiming to improve performance, dependability, and cut down costs. The packaging of MEMS sensors can constitute up to 30% of the cost of producing a device[1], the sealing capacity and interconnectivity significantly impact device performance, which subsequently affects the production and application of sensors. Wafer-level packaging has advantages in reducing the size and saving costs compared to device-level packaging, exhibiting manufacturing efficiency and excellent device performance[2].

TGV (Through Glass Via) is the vertical electrical interconnection through the glass substrate, which corresponds to TSV. Glass substrates possess superior electrical properties and lower parasitic capacitance than commonly silicon and SOI substrates, facilitating extending for high-frequency signal transmission[3]. The excellent optical properties of glass make it more suitable for optical applications such as Micro-Opto-Electro-Mechanical Systems (MOEMS) [4]. Adjusting the composition of the glass and optimizing surface treatments can modify the coefficient of thermal expansion (CTE) and mechanical strength of the substrate. This results in improved metal adhesion, stress control, and reliability[5,6]. TGV technology supports a wide range of thicknesses (50um-900um) and large wafer sizes (6″-12″) and panels (510×515mm-1500×800mm). The glass-based process is more straightforward without the need to deposit an insulating layer on the inner wall of the TGV, making the manufacturing cost of glass package substrates much lower than that of silicon substrates. Glass can be bonded to substrates, including silicon and other glasses using techniques such as anodic bonding and direct bonding. These methods create a stable vacuum environment suitable for inertial sensors like accelerometers and gyroscopes[1,2,5,7-11]. The TGV process provides

 doi:10.20944/preprints202312.0064.v1

the fabrication and metallization of high-density, high-aspect-ratio glass vias, enabling a reduction in device size while maintaining high-performance electrical interconnects. Intel says glass substrate technology can increase the chip area in a single package by 50 percent, allowing more chiplets to be crammed in. It reduces the thickness by about half compared to ABF plastic, providing higher signaling speeds and power efficiencies.

There are many reports and studies on TGV. However, fewer introductions and summaries are provided on applying TGV technology in the field of sensors. The critical processes of TGV technology are glass via formation and via metallization. Among them, there is a more significant amount of review literature on glass via processing, while there are limited reviews on via metallization. This paper presents an overview of the research progress in TGV fabrication, which encompasses glass via formation and metallization, considering the advances and findings accomplished by the scientific community. The applications of TGV technology in sensors are reviewed, and the current challenges and prospects of TGV are examined.

2. Through-glass-vias Formation and Metallization Techniques

Glasses, including quartz, borosilicate, soda-lime, and high-alumina glasses, primarily consist of silica and other oxides. There is a variety of options for glass substrates in terms of their size, thickness, and material properties, but only particular types, such as ultra-large (>2m × 2m) and ultra-thin (< 50μm) panel glass, as well as thin and flexible glass materials, are solely provided by major glass manufacturers, including Corning, Asahi, and SCHOTT. Different TGV processes can process a variety of substrates, thicknesses, and apertures. In wafer-level packaging, high-quality borosilicate or quartz glass is commonly used as a substrate with micro-perforations having a diameter ranging from 10μm to 100μm and an aspect ratio ranging from 1:1 to 70:1. For certain sensor packaging and manufacturing purposes, larger sizes (>300μm) and lower aspect ratios (<1:1) may still fulfil the required criteria.

As stated earlier, the primary processes involved in TGV technology are forming and metallization of vias. This section presents established methods for through-hole formation in glass, such as abrasive jet micromachining, electrochemical discharge machining, laser ablation, and photosensitive glass methods. Details of each processing method are provided, including the process principle, pore-forming capability, and the type of glass that can be processed. Each process is introduced with principle, ability, and research advancements for through-hole metallization technology based on glass through-hole forming technology.

2.1. Through-glass-vias Formation Techniques

2.1.1. Abrasive Jet Machining (AJM)

Abrasive jet machining is a non-conventional process whereby the surface is treated using abrasive jet to create a specific surface shape[12-24]. The AJM process typically uses abrasives such as Al_2O_3, garnet, SiC, or diamond particles and has the capability to handle a diverse range of substrates such as metals, glass, ceramics, polymers, and composites[17,20]. The AJM process is suitable for processing large-sized and high-thickness substrates. It can create blind grooves, blind holes, through-hole structures or polish the surface of the material[21]. Localized processing and protection of non-processed areas are typically accomplished by depositing a particle resistant metal or polymer mask on the surface of the substrate[13]. AJM is a comparatively cost-effective and accurate alternative to conventional machining techniques. The non-thermal machining method does not affect material properties and can be used in non-dust-free environments. It is widely used in semiconductor manufacturing, electronic devices, microfluidic channels and microelectromechanical systems (MEMS)[14].

The AJM process using doped abrasives can be classified into three categories based on the type of flow medium involved: abrasive slurry jetting, abrasive water jetting and abrasive air jetting. Abrasive air jet machining is also known as sand blasting and powder blasting[25]. There are variations in abrasive flow patterns between air and slurry/water-based systems, but their erosion

 doi:10.20944/preprints202312.0064.v1

patterns within the glass are similar, relying primarily on brittle erosion to produce cracks and debris to remove material[18]. Processes that employ slurry as the flow medium boast a relatively small erosive footprint owing to the concentrated spray area, low impact of collisions between the abrasives. However, the jet decelerates quickly before reaching the substrate's surface. At the same jet pressure, the erosion rate of ASJM is significantly lower than that of AJM[18].

AJM's research in the field of glass cutting and drilling is relatively mature. Al_2O_3 is the primary abrasive used, with particle sizes ranging from 5μm to 100μm, with smaller abrasives being used to achieve lower in-hole roughness. The abrasive is propelled by compressed air, water or slurry and comprises 1-8.2% of the mass of the jet. Impact angle, jet pressure, nozzle distance, nozzle inner diameter and mass percentage of abrasive in the jet constitute the main process parameters[12]. The duration of processing a single hole takes a few seconds, with the processing speed ranging between 0.1μm/s to 32μm/s in an air environment and 0.6μm/s to 4.4μm/s in a slurry environment. It is possible to improve efficiency by processing a mask and using multiple nozzles in parallel[25]. Holes with a diameter ranging from 0.3mm to 6mm can be produced with a maximum aspect ratio of approximately 5:1. The jet injects from one side, resulting in tapered holes with a greater diameter on the inlet side and a lesser diameter on the outlet side. Accurate alignment and symmetrical machining of both front and back sides permit a double conical through-hole. The shape of the bottom of the blind aperture is influenced by the air flow pressure and particle velocity, resulting in a concave (U-shaped), flat, or convex (W-shaped) structure[13,23]. Direct drilling without a mask produces a hole that is nearly four times wider than the diameter of the jet, the mask influences the bottom shape of the hole and reduces the frosted areas around the hole[19]. Ultrasonic vibration-assisted abrasive waterjets (UV-ASJ) enhance drilling performance by inducing a brittle-ductile transition mechanism that enables the material to detach from the target in a desirable manner. Additionally, UV-AJM, along with small abrasive sizes and low kinetic energy, facilitates uniform drilling that minimizes W-forms, diminishes surface roughness and improves drilling efficiency[24]. Overall, the AJM technique is better suited for processing low aspect ratio holes in large-size thick glass substrates. The research on the hole formation principle and drilling model is relatively advanced. However, it is difficult to produce holes quickly and the roughness inside the holes is high and not flat enough, which makes it difficult to achieve metallization.

2.1.2. Electrochemical discharge machining (ECDM)

Electrical discharge process using breakdown and high pressure to generate heat to cause the glass to melt locally to form vias[26]. Vias are fire polished to a very smooth inner wall and residual stresses are removed by post processing annealing. The method can drill vias in fused quartz, soda-lime, and non-alkali glass without requiring a mask or dust-free environment. The method is more efficient than machining, completing each via in just 200-500ms, and can be executed simultaneously through numerous discharge ports. It is possible to drill vias in glass with a thickness of 100-500μm. Because thick glass produces more molten glass splash during drilling, 100-200μm thin glass is preferred and can be bonded to 500μm carrier glass. The electrical discharging method allows for a high degree of process freedom, enabling the processing of small, fine-pitch via arrays. Vias with a diameter of 20μm and a spacing of 60μm can be fabricated on thin glass, while top 60μm and bottom 40μm vias can be produced on thick glass.

Electrochemical discharge machining, or spark-assisted chemical engraving (SACE), is a machining technology that hybridizes electrochemical machining and electrical discharge machining[27-37]. The ECDM method can achieve parallel processing of large-area vias arrays by customizing the working electrode, inheriting the high cost effect and process flexibility of the EDM method. The diameter and morphology of vias processed by ECDM are related to the size and surface roughness of the tool electrode. When the electrode size and surface roughness decrease, the size of the air film on the electrode surface, the heat affected zone and overcut decrease[30]. The average material removal rate was 3μm/s for drilling and 50μm/s for machining the slot. the electrode widths used ranged from 80μm-150μm, and drilling typically involves an overcut of 150-300μm on the front side and 100-200μm on the back side, resulting in a lower limit of 280-300μm for vias[35]. By adding

Preprints (www.preprints.org) | NOT PEER-REVIEWED | Posted: 1 December 2023 doi:10.20944/preprints202312.0064.v1

magnetic stirring to the discharge process, the bubble aggregation and erosion effects can be optimized, resulting in an increase in the aspect ratio of vias and a reduction in the heat affected region[37]. Electrochemical discharge method is a low cost, small scale process. However, the drilling rate is slow and the process is random. It is difficult to achieve a vertical shape in the hole and the presence of heat affected areas affects reliability.

2.1.3. Photosensitive Glass

Alkali and alkaline-earth metal oxides are added as cosolvents to SiO_2 glass, along with metals like Al and photosensitive active ingredients like Au and Ag, to produce photosensitive glass. Reactions occur within the photosensitive glass after exposure to light of specific wavelengths. Subsequently, the glass undergoes permanent property modifications after being exposed to heat treatment. Chemical etching enables the production of glass microstructures[38]. Commonly used photosensitive glass, such as Schott's FOTURAN II photosensitive glass, undergoes a photochemical reaction to release free electrons when exposed to UV light. Heating the glass to 500-600°C causes doped Ag+ within the glass to absorb electrons and convert into silver atoms, becoming a nucleation center to develop lithium metasilicate crystals (Li_2SiO_3). The hydrofluoric acid etching rate of Li_2SiO_3 reaches 20-50 times higher than that of the unaffected zone, enabling selective etching of the glass and unveiling microstructures like vias[39].

Photosensitive glass can be modified by UV laser irradiation or maskless modification. Both processing methods allow the formation of vias with aspect ratio of more than 8:1 (e.g. 25:1-35:1)[40-42], with good perpendicularity (inclination as low as 1°) and roughness (less than 1μm) of the inner wall of the vias[43] as illustrated in Figure 1[43]. Brokmann et al.[44] processed glass by plasma etching and compared it to wet etching methods, demonstrating that plasma etching offers new degrees of freedom in microstructure control and microsystem fabrication. Photosensitive glass shows promise for high-density interconnection and microsystem integration, but faces challenges such as the high cost of photolithography and laser-induced processes, the high cost of glass, and the complexity of processing.

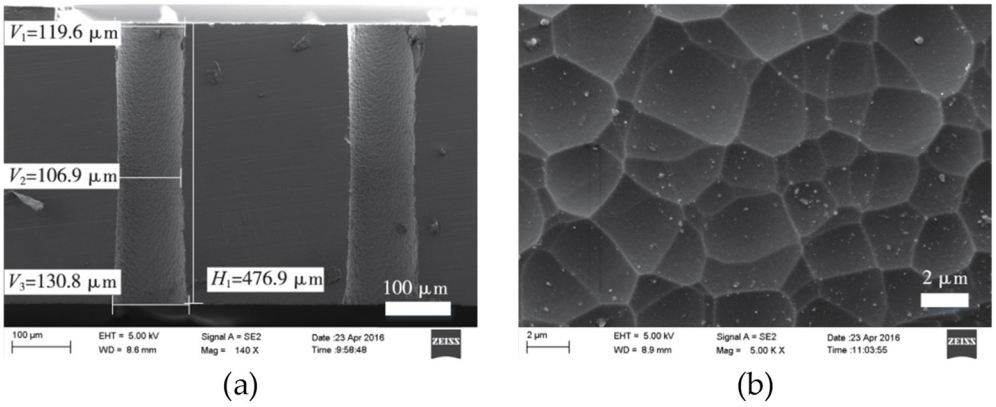

Figure 1. SEM image of photosensitive glass via after wet etching (a) cross-sectional view (b) surface view of inner wall[43].

2.1.4. Glass Reflow Process

The glass reflow process capitalizes on the liquidity of molten glass, enabling its flow into reserved spaces to forge the intended structure [45]. The process typically employs Deep Reactive Ion Etching (DRIE) to treat the silicon substrate and create a reverse structure. The silicon substrate is then anodically bonded to the glass substrate, resulting in a confined cavity. Afterward, the bonded wafer is heated to melting temperature in an annealing furnace, and the molten glass is drawn into the silicon cavity until the space is completely filled with glass as shown in Figure 2[46]. The silicon-glass substrate is created by thinning and polishing the reflowed substrate to remove a specific

Preprints (www.preprints.org) | NOT PEER-REVIEWED | Posted: 1 December 2023 doi:10.20944/preprints202312.0064.v1

amount of glass and silicon on either side. Glass microstructures, such as rings, gears, tuning forks etc., may be produced using the glass reflow technique [47]. In the realm of wafer-level packing, low-resistance silicon can be depended on for vertical electrical connections while glass provides signal insulation and device protection[48].

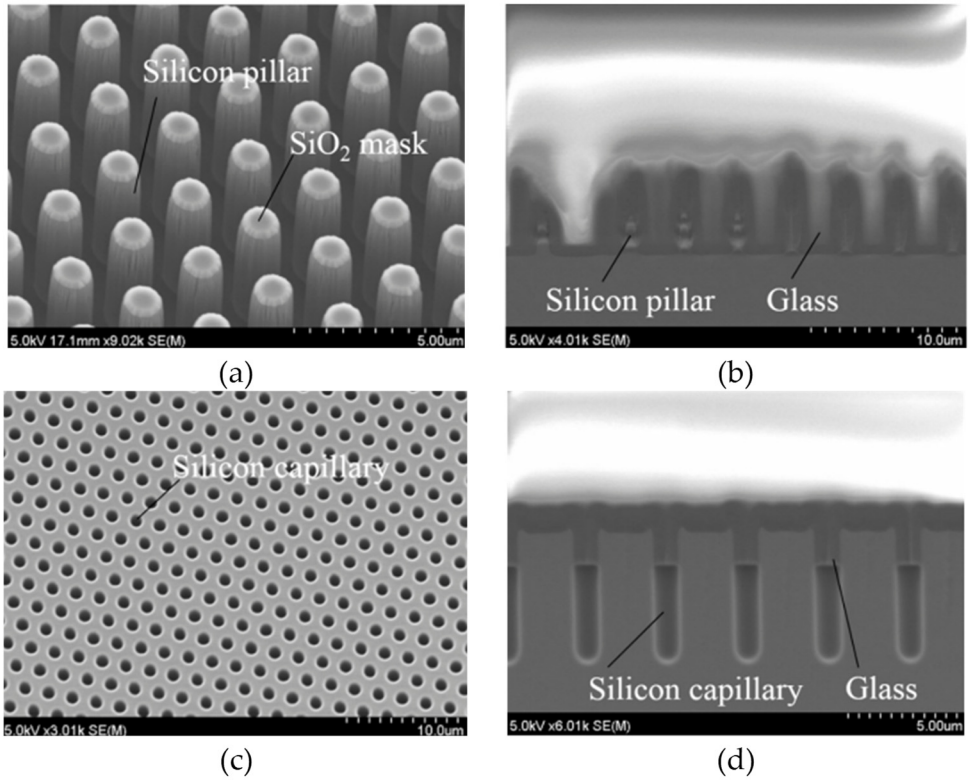

Figure 2. Glass reflow process into small cavities. (a) Silicon pillar mold ; (b) silicon capillary mold,(c) penetration depth of pillar mold under third reflow condition ; (d) penetration depth of capillary mold under third reflow condition[46].

The glass reflow technique has been applied in the fabrication of glass micro lens arrays [49] and hermetically sealed integrated silicon through-mechanical sensors [50]. The study by Haque et al [45] employed the glass reflow process to produce package substrates suitable for hermetic sealing and galvanic isolation, demonstrating the viability of the process for use in capacitive pressure sensors and hermetically sealed resonators. Toan et al [46] addressed the difficulty of filling tiny scale patterns with glass and investigated the phenomenon of glass reflux into large cavities, microgrooves and microcapillaries. They demonstrated that the addition of a 50 nm SiO_2 film on the surface of a silicon substrate can enhance the surface's wetting properties with glass. Due to the confined space and high surface tension present in microcapillaries, filling the glass is challenging. Extending the reflux time helps enhance the filling capacity of reflux[51]. Li et al [52] employed a double-sided reflow procedure to address the cavity formation issue that arises after glass reflow. Meanwhile, Liu et al[53] utilized nano-glass powder as a substitute for glass substrate to enhance the filling effect and prevent the anodic bonding and thinning process. Nguyen et al [54] used glass reflow to fabricate CMUT arrays, proving that the process can be applied to optical microfluidics, 3D-MEMS, etc. Kuang et al [2,10,11] created TGVs in a silicon substrate using the glass reflow method. The triple anodic bonding of the TGV substrate, the MEMS structure and the glass cap completed the wafer level vacuum packaging.

 doi:10.20944/preprints202312.0064.v1

2.1.5. Laser Ablation (LD)

Mechanical techniques including the abrasive jet machining method make it difficult to form vias less than 100μm in diameter. In contrast, laser ablation presents an effective means of creating low diameter and high depth-to-width ratio vias by forming micro-vias through thermal shock and ablation[55-66]. Lasers have widespread applications in cutting and drilling various materials, including PCB substrates. Research on laser processing of glass substrates is highly developed. Commonly employed lasers for glass substrate processing include infrared CO2, ultraviolet UV-YAG and ArF excimer lasers. Laser ablation is a production process that requires no mask and enables quick processing, making it suitable for mass production. Yet, challenges such as heat-affected area expansion, hole thermal damage, and the emergence of protrusions near vias edges impede bonding[57]. Optimization can be achieved by various means, including the addition of an organic layer on the glass surface to reduce laser damage, immersion of the glass in a cooling liquid to decrease the thermal impact, preheating the glass before processing, or the use of shorter pulse lasers.

The absorption rate of glass in the visible range is low, UV and IR lasers prove to be more efficient for glass processing[65].However, even within the visible range, ultrashort pulsed lasers such as picosecond and femtosecond lasers can be used to create vias by enhancing the absorption of glass through multiphoton absorption. The non-thermal processing of short pulsed lasers mitigates thermal damage within the glass, though the development of stress waves can create microcracks in the internal wall of the hole[60]. CO2 lasers have long been one of the most commonly used lasers in industry due to their relatively low cost and simplicity of equipment.CO2 lasers are capable of producing vias with diameters of less than 100μm and spacing of 400μm on 500μm Schott D263Teco glass[56]. The CO2 laser is capable of achieving through-hole fabrication on a 140um thick polymer laminated glass with an incident surface diameter of 120um and an output surface diameter of 75um[62].

The processing speed of picosecond lasers is 500 times faster than that of CO2 lasers, reaching 10m/s. After a latency period of about 1μs, the glass reaches the threshold temperature by multiphoton absorption, at which the irradiated material is rapidly heated by linear absorption to form vias with a diameter of 10-20μm[65]. Using liquid-assisted laser processing, CO2 lasers are capable of producing arrays of vias ranging from 100-200μm without any crack or burn zones when operated at 6W power with a scanning speed of 11.4mm/s [55]. In order to avoid defects of 500μm damage zone, picosecond lasers utilize liquid-assisted processing. It has been demonstrated that machining 100μm diameter vias in 800μm thick glass can be achieved with a reduced heat affected zone of 15μm and a reduced taper of 2μm[64]. The addition of a PDMS protective layer to the glass surface reduces the thermal effect on the glass surface bumps from 15.1μm to a minimum of 1.2μm[57].

2.1.6. Laser Induced Deep Etching(LIDE)

Several previously discussed drilling methods have problems such as the inability to process small holes, poor accuracy, and cracking. To address such shortcomings, LPKF put forth a high-precision, low-cost laser-induced deep-etching (LIDE) technique [67]. Use a picosecond laser to process a glass substrate to form induced areas with diameters of approximately 1 μm [68]. Place the glass in hydrofluoric acid or alkaline solution, the etching rate of the laser-induced areas is much higher than other areas of the glass, the laser-induced region is enlarged to form vias and remove thermal damage. LIDE is suitable for processing vias or arrays of blind holes of arbitrary size and spacing. It is capable of creating cavities of any shape or large vias by closed connecting closely spaced vias (1-10 μm) [69].

The LIDE method is recognized as a highly potential technology for TGV production [70]. LIDE is well researched [71-74] and has been extensively adopted by industrial players, including Corning, Schott, AGC, Mosaic Microsystems, LPKF, Plan Optik, Samtec, and Sky-semi. Typical glass vias exhibit an hourglass shape with diameters ranging from 20 μm to 100 μm and substrate thicknesses ranging from 50 μm to 1 mm. Aspect ratios typically range from 10:1. Glass vias feature smooth sidewalls (Ra < 0.8 μm) without cracks and taper angles ranging from 0.1°-30° [75]. The glass surface

Preprints (www.preprints.org) | NOT PEER-REVIEWED | Posted: 1 December 2023 doi:10.20944/preprints202312.0064.v1

is smooth after etching, with roughness less than 20 nm. The etching rate of the alkaline is lower compared to that of the acid; however, the induced region's selective etching nature is better, allowing the formation of near-vertical vias with high aspect ratios. Quartz glass and borosilicate glass show higher selective etching ratios than other glass types[76]. It is possible to process glass vias with diameters less than 7μm and aspect ratios as high as 50:1, 70:1, and even 100:1. Integration of vias and blind holes with different diameters on the same glass substrate can be realized by multiple LIDE processes, or cavity-vias structures as shown in Figure 3. LIDE process takes longer to process large-size cavities. It requires machining blind holes with set point spacing, which are connected to form cavities. The processing time of cavities depends on the laser-induced dot spacing and the laser travel speed. The larger the dot spacing, the higher the roughness at the bottom of cavities (Ra > 0.1μm), while too small dot spacing can cause heat build-up problems inside the glass during laser induction, affecting the processing results. LIDE method has multiple advantages in speed, quality and cost. It can process wide ranges of TGVs with high compatibility with other processes, which has high potential for application in the fields of 3D integration and wafer-level packaging.

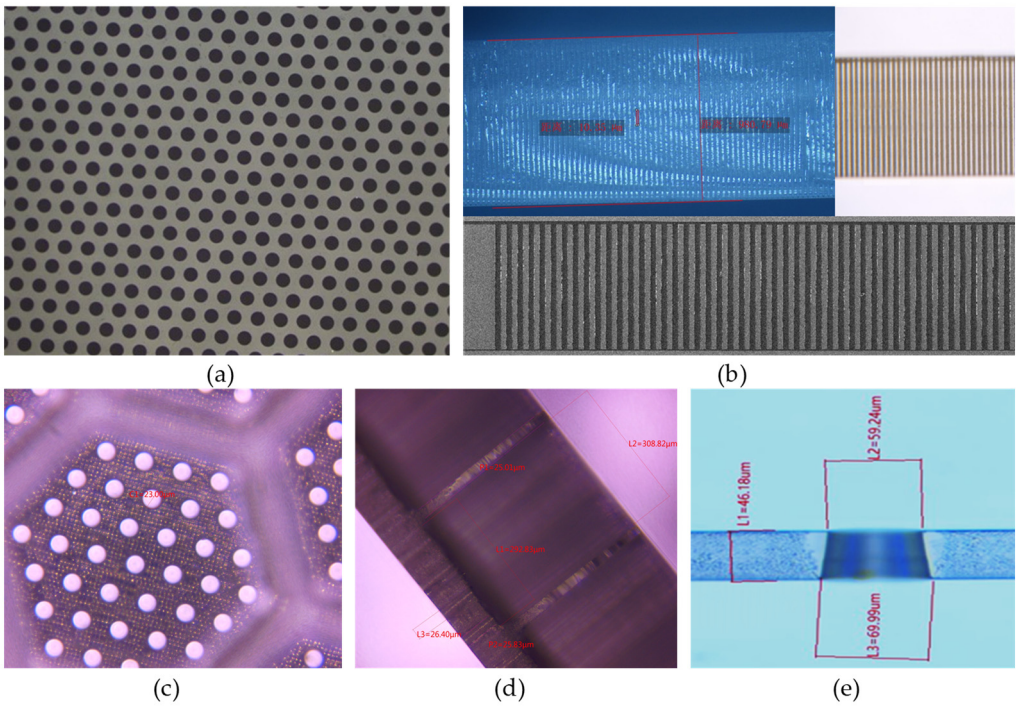

Figure 3. TGV samples processed by Sky-semi (a) the top view of glass through-hole array ; (b) the cross-sectional view of ultrahigh aspect ratio(50:1-100:1) glass vias ; (c) the top view of blind slot-vias structure ; (d) the cross-sectional view of blind slot-vias structure ; (e) the cross-sectional view of trapezoidal via.

2.2. Through-glass-vias Metallization Techniques

2.2.1. Conductive Paste Filling Method

Metallic conductive pastes offer adjustable CTE and can be bonded directly to glass, compatible with the TGV process. The conductive pastes can be filled physically into vias and sintered to construct electrical interconnects. Nano-silver paste and conductive copper paste can be chosen as materials for filling vias. Filling the pastes by vacuum plugging or 3D printing requires no complex equipment or process to achieve high aspect ratio and density vias arrays. There may be a volume reduction of the paste after curing resulting in dishing in vias(5-20μm depends on via diameter and substrate thickness) in the vias, which can be removed by refilling the paste or thinning the glass substrate. There remains a residue on the surface of the glass after the printing and filling process.

Preprints (www.preprints.org) | NOT PEER-REVIEWED | Posted: 1 December 2023 doi:10.20944/preprints202312.0064.v1

After sintering, it is necessary to polish the front and back of the glass to enhance its surface cleanliness.

Takahashi et al [26] achieved the filling of conductive copper paste inside 50μm diameter, 130μm pitch TGVs, where the resistivity of the copper paste was about 1.6-1.9Ω·m/sq. We successfully filled 50μm and 100μm diameter vias on a 400μm thick BF33 glass substrate using conductive silver paste. Then, we processed daisy chain and coplanar waveguide to analyze the interconnect performance. The vias filled are free of defects such as air bubbles, and the resistivity of the silver paste inside the vias is $2.56 * 10^{-7}\Omega\cdot m$. The conductive paste has the potential to attain an aspect ratio exceeding 10:1 for sealing vias and interconnections, as well as filling vias ranging from 50μm to 1mm in diameter, thereby making it an economical and high-performance metallization technique as illustrated in Figure 4. However, the glass surface needs to be thinned after the paste is sintered, leading to reliability issues with the glass. The conductivity of the paste is low and its resistivity varies during the sintering process. Therefore, the conductive adhesive filling method is suitable for applying TGV metallization with low electrical interconnect standards or very high aspect ratios, but the process stability still needs to be improved.

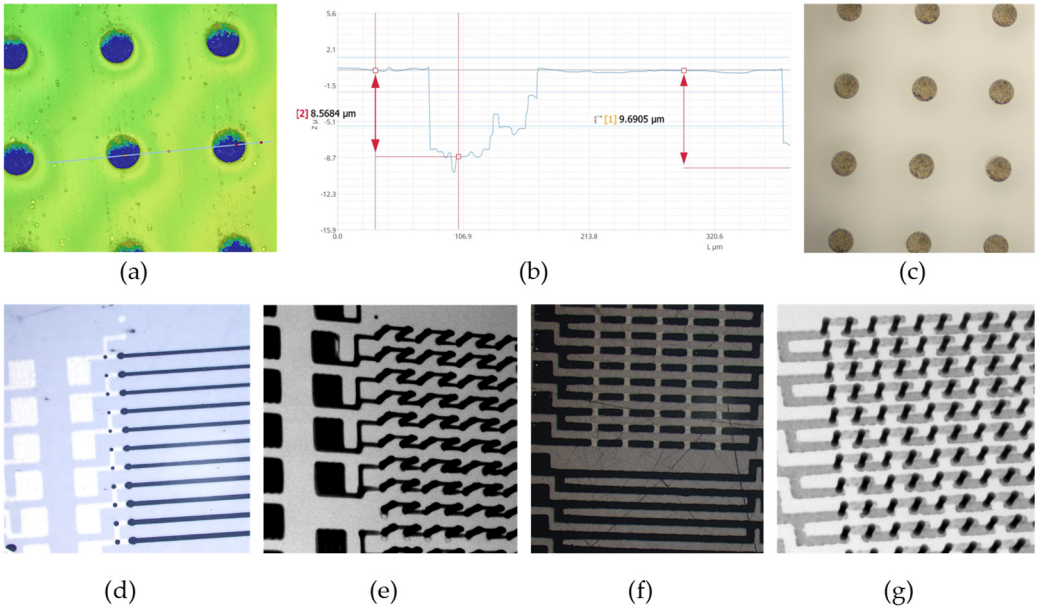

Figure 4. (a) the 3D images of paste filled vias; (b) dishing of the paste filled vias before thinning ; (c) the top view of paste filled vias after thinning ; (d) the OM image of daisy chains using 3D printing to fill vias and surface wiring ; (e) the X-Ray image of daisy chains using 3D printing to fill vias and surface wiring (f) the OM image of daisy chains using vacuum plugging to fill vias and surface wiring(thinning causes cracks in the glass) ; (g) the X-Ray image of daisy chains using vacuum plugging to fill vias and surface wiring.

2.2.2. Magnetic Self-assembly Method

The widely utilized super-conformal electroplating process presents challenges in filling vias with rough sidewalls and poor hole wall morphology. The optimization of via filling for diverse aspect ratios and tilt angles is challenging. Therefore, Laakso et al [77] proposed a solution to fix the nickel wire inside the glass vias using magnetic field assisted self-assembly to achieve electrical interconnection.

Cut nickel wires can be loaded magnetically into the glass vias. The vias were filled with Spin-on-glass and cured with methyl siloxane. The voids in the vias were refilled due to shrinkage, and the magnets were removed from the bottom of the substrate. The SOG was cured, and after the front-side wiring had been completed, a backside wet etch was used to thin the wafer and remove the nickel wire, thus finalizing the glass vias metallization process. This method enables the metallization

Preprints (www.preprints.org) | NOT PEER-REVIEWED | Posted: 1 December 2023 doi:10.20944/preprints202312.0064.v1

of TGVs with high-density, high aspect ratio, and low resistance value while ensuring compatibility with various inner wall morphologies and roughness vias. Adjusting the composition of metal rods and SOGs can mitigate the thermal mismatch problem in TGVs. The process has strict requirements for magnetic control, which may require multiple magnets to completely fix the wires inside the vias, and the length of the magnetically controlled wires must be greater than the width to achieve proper orientation. However, using the HF etching approach to thin the wafer for exposing the nickel wires poses a challenge with the etchant penetrating the sidewalls of the SOG and TGV vias. To overcome this, a mechanical mask can be implemented with CMP, which does not affect the thinning capability.

2.2.3. Electroplating Method

Like the use of electroplating technology to fill TSV structures, metal can also be deposited into TGV structures through electroplating. As illustrated in the Figure 5, the specific process[78]is: (1) deposit diffusion barrier layer and seed layer in TGV pores by physical vapor deposition (PVD) and other methods; (2) fill the required metal from bottom to top by electrochemical reactions, usually by electroplating Cu; (3) remove excess Cu from the surface by methods such as wet corrosion and CMP. The bottom-up plating technique initiates from the hole's bottom, preventing void formation during filling. However, the process is time-consuming and costly. Subsequently, partial filling methods have been introduced, also recognized as conformal filling. The TGV hole does not necessarily require complete filling. Instead, it can be filled along the sidewall or a semi-enclosed structure, such as a copper bridge[79], to improve electrical connection. A resin film can laminated as an insulation layer in the TGVs[80]. Partial filling technology can be compared to full filling technology in terms of electrical performance[81], and the electroplating time and costs have been optimized to some extent.

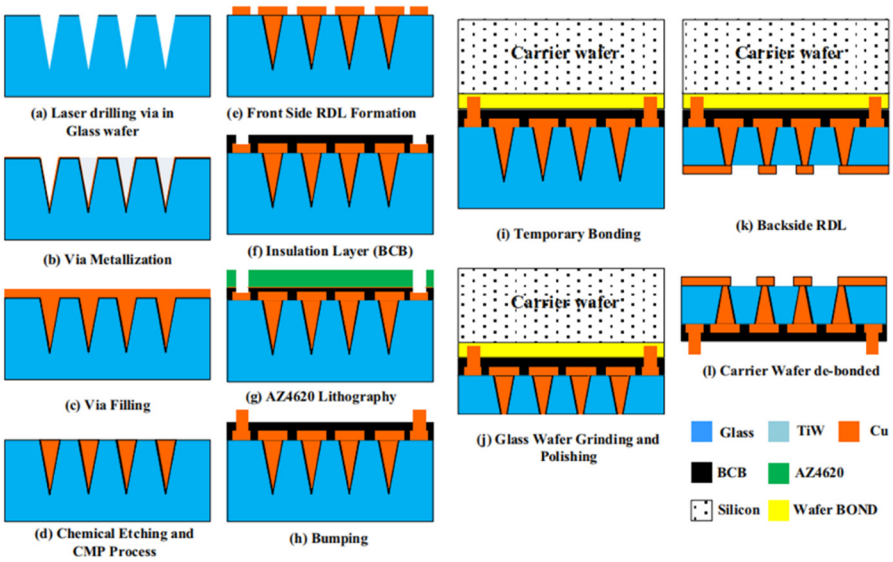

Figure 5. Schematic fabrication process for glass interposer[78].

ALD demonstrates superior microporous filling performance compared to PVD and can be effectively utilized in the TSV process to deposit insulation, barrier, and seed layers. Blind silicon vias with a 3μm diameter and a depth of 50μm (aspect ratio 15:1) can be filled using chemical plating and electroplating[82-87]. We deposited Ru as a seed layer and achieved defect free filling of small silicon blind holes as small as 3um in diameter and 45um in depth. We achieved blind glass vias electroplating with aspect ratios of 7:1 and double-sided TGVs electroplating with aspect ratios of 4:1 as illustrated in Figure 6. Lee et al.[88] achieved a bottom-up electroplating process without seed layers to achieve pore free filling of TGV holes with high aspect ratio and smooth sidewalls, and vertically interconnected RF MEMS devices. In order to achieve a seedless electroplating process, they use low resistance silicon as the substrate, and the etched silicon surface can act as a seed layer. Tanaka et al[89] plated TGV vias with a depth of 300μm, a diameter of 60μm at the bottom, and a

Preprints (www.preprints.org) | NOT PEER-REVIEWED | Posted: 1 December 2023 doi:10.20944/preprints202312.0064.v1

diameter of 40μm at the top to achieve partial filling, and investigated the feasibility of conformal filling through the simulation analysis of the current distribution. In coplanar waveguides (CPWs) prepared on this basis, the insertion loss due to TGV is 0.2 dB at 30 GHz, and therefore the transmission line using TGV can be used for high-speed signal transmission using high-frequency frequency bands. Wang et al[6] realized X-shaped partially filled TGVs and RDLs by a double sides Cu conformal electroplating process. No cracks or protrusions (cracks or protrusions) were observed at critical locations in 100 thermal cycling experiments between -40°C and 125°C. This indicates that the electroplating-filled TGV process has a good application prospect for the preparation of MEMS devices.

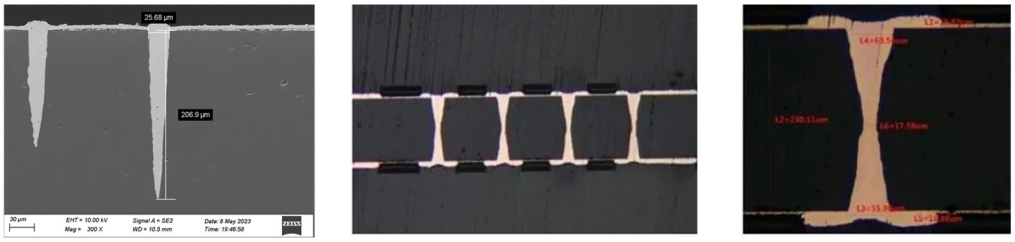

(a) (b) (c)

Figure 6. Cross-sectional SEM photos of (a) electroplated filled blind glass vias, (b) and (c) Electroplated filled TGVs.

3. Application of TGV for sensors manufacturing and packaging

Packaging serves to isolate sensitive and fragile internal and external environments, protect internal space, and facilitate signal transmission. The cost of packaging MEMS sensors accounts for more than 30% of the total manufacturing cost. The optimization and enhancement of the packaging process can assist the sensors in achieving superior performance whilst reducing costs.

The packaging process is essential for sensors, particularly MEMS sensors. Wafer bonding technology and vertical interconnect technology are the key technologies for wafer level packaging technology, which is of great value in achieving smaller device size, lower manufacturing cost and lower power consumption[10]. Glass has been widely used in sensors packaging due to its unique properties such as high mechanical stability, high sealing performance, high transparency and low thermal conductivity. It can serve as a cap substrate to create a highly vacuum-sealed environment through anodic bonding, direct bonding, or metal bonding with silicon, SOI, glass, or other substrates in sensor packaging. Moreover, the development of TGV technology mainly including vias formation and metallization has made glass substrates more preferred in sensor packaging due to their superior performance advantages. As shown in Figure 7, this section provides detailed information on the application and performance of the TGV process for different types of sensors according to the performances of glass.

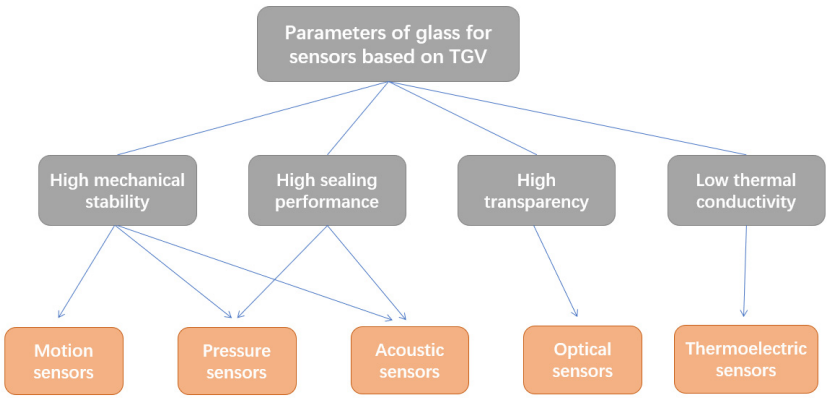

Figure 7. Parameters of glass for sensors based on TGV technology.

 doi:10.20944/preprints202312.0064.v1

3.1. Motion Sensors

Motion sensors are typically used for motion detection and acceleration measurement. Chips require sufficient impact resistance to protect the internal microstructure. Glass has strong mechanical properties that can improve the impact resistance of sensors. TGV technology has great potential for motion sensing applications.

Ma et al[5] used a glass adapter plate as a top cover to solve the stress problem of TSV technology. A symmetrical sandwich structure for MEMS inertial sensors based on bulk silicon process was constructed. Blind vias were formed on a 400μm thick glass substrate by powder blasting and TGVs were formed by backside grinding and polishing. Al was deposited by sputtering to provide electrical interconnections in the TGVs. A redistribution layer is formed on both sides of the adapter plate by photolithography. BCB is used as an adhesive layer to bond the adapter plate to the MEMS accelerometer wafer for wafer-level packaging of the accelerometer.

Fu et al [7] proposed a comb structure accelerometer in which the glass cover plate with TGV is bonded to the accelerometer anode to form a sealing and interconnection structure. Laser ablation was used to create square vias with 300μm thickness on BF33 glass. The TGV metallization process was performed using metal mold method [90]. Yang et al [8] used the powder blasting method to fabricate biconical vias with a diameter of about 600μm on a 500μm thick glass substrate. Cr/Cu was sputtered onto the substrate as a seed layer, which was then filled with TGVs through a PPR copper plating process. Following polishing, the TGV substrate was obtained from which shock threshold sensors were fabricated. During testing, reliable switching signals were obtained at a shock velocity of 1000g.

Yang et al.[2] processed Pyrex 7740 glass using a picosecond laser at a wavelength of 532nm and obtained vias with an entrance diameter of 90μm, an exit diameter of 48μm and a depth of 300μm. Vertical electrical interconnections were achieved using electron beam evaporated metal filler to cover the inside of the TGV, and the TGV substrate was bonded to the gyroscope to complete the package. The devices were tested to maintain a vacuum of 1 Pa for over two years. Zhang et al.[9] fabricated glass caps with low-resistance silicon as conductive column using a glass reflow process and completed the hermetic encapsulation of the capacitive gyroscope by anodic bonding. The quality factor of the tested device exceeds 220,000, which is an order of magnitude greater than that of the unencapsulated gyroscope. Kuang et al.[2,10,11] conducted an initial investigation into the process mechanism of glass reflow, followed by the successful sealing of a gyroscope using this method. This proved the feasibility of wafer-level vacuum packaging using TGV technology in combination with triple-anode bonding.

3.2. Pressure Sensors

Pressure sensors can be categorized as capacitive pressure sensors, piezoelectric pressure sensors, or resonant pressure sensors, which can be used in aerospace inspection and atmospheric pressure sensing. These sensors are typically vacuum sealed, such as micro resonators, where the mechanical quality factor deteriorates with increasing ambient pressure due to air damping effects. The potential of the TGV process for applications such as capacitive pressure sensors has been demonstrated. Haque et al[91] produced capacitive pressure sensors using glass reflow method. The wafer was heated inside a tube furnace and the grooves were filled with melted glass to form silicon conductive vias. This process completed the sealing of the sensor and provided electrical lead-in, eliminating the need to install bond wires on the front.

Kim et al[45] used glass reflow technology to fabricate silicon-glass structured wafers for electrical interconnects, proved that glass provides good electrical isolation and minimizes parasitic capacitance. Zhenyu et al. [92] used laser drilling in Pyrex 7740 glass to fabricate glass caps. The resonant pressure sensors were fabricated by combining glass caps with TGVs on SOI wafers. The glass cap with TGV achieved both vacuum sealing and electrical lead-out. The micro-pressure sensor manufactured was verified to have a Q-factor greater than 22,000 and was stable for 5 months, confirming the reliability of the vacuum package and electrical connection.

Preprints (www.preprints.org) | NOT PEER-REVIEWED | Posted: 1 December 2023 doi:10.20944/preprints202312.0064.v1

3.3. Acoustic Sensors

The changes in external environment (such as temperature, pressure, humidity, etc.) have an impact on the properties of sensor materials, thereby affecting the propagation characteristics of sound waves (mainly the sound speed). By utilizing this principle, changes in sound speed can be detected to determine changes in the external environment.

Chen et al [101] designed a new three-dimensional wafer-level packaging (3-D WLP) solution to improve the performance and reliability of surface acoustic wave (SAW) filter packages with large cavities. Glass capping and vertical interconnects were realized using TGV, which can avoid the outgassing problem and prevent the contamination of the interdigital transducers (IDTs).

The application of TGV technology in acoustic sensors is still relatively limited, mainly focusing on CMUT. Ultrasonic transducers have potential applications in the medical and underwater exploration fields [93]. Capacitive micromachined ultrasonic transducers (CMUTs) offer an alternative to piezoelectric technology for producing two-dimensional ultrasonic transducer arrays with typical integrated circuit manufacturing processes. CMUT arrays can be integrated with front-end ICs through flip-chip bonding and TSV processing. TSV processing is a complex procedure with high parasitic capacitance and roughness, which can cause additional stress and degrade CMUT performance. As a result, TGV technology presents itself as a promising alternative.

Zhang et al [94] developed a procedure to create vacuum-sealed CMUTs through anodic bonding on borosilicate glass substrates. They then extended this process using TGV interconnects. Laser ablation was employed to generate via holes, with 70μm diameter at the entry and 50μm at the exit on 700μm thick borosilicate glass. Copper paste was used to fill the vias, which were subsequently sintered and polished to form the TGVs. CMUT array fabrication was completed and performance tests were conducted to demonstrate the devices' basic functionality, although they were not vacuum sealed. Zhang et al [94-97] reported a fabrication process for vacuum-sealed CMUTs on borosilicate glass substrates using anodic bonding and completed the fabrication process as shown in Figure 8. A process of fabricating using sacrificial etching was demonstrated to overcome the restriction of employing glass substrates that are compatible with anodic bonding.

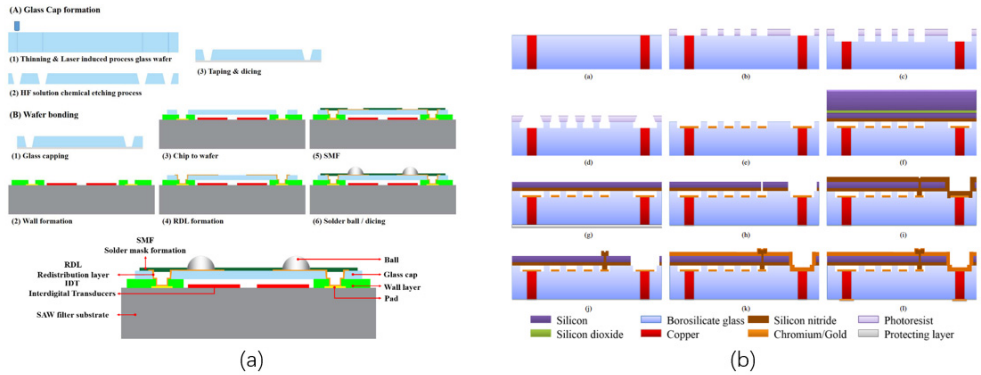

Figure 8. the fabrication and packaging process of acoustic sensors based on TGV technology: (a) SAW filter[98]; (b) CMUT [94].

3.4. Optical Sensors

There are still limited optical components and systems utilizing the wafer-level packaging method. Glass, which has remarkable optical and electrical characteristics, is particularly appropriate for packaging optical sensors. Brusberg et al [99,100] used a laser drilling process to fabricate TGVs in D263T glass for 3D interconnections, and integrate Mach-Zehnder interferometer (MZI) waveguides, fluidic channels, optoelectronic elements, and silicon dies to form optical sensor. Stenchly et al [4] introduced a modular packaging system suitable for optical components and systems. The system comprises a TGV interposer and a glass cover plate. A specialized process can fabricate an optical window on the glass cover plate, achieving tilting by way of structural tilting

 doi:10.20944/preprints202312.0064.v1

through thermally induced stresses during high-temperature baking. TGV adaptor plates can be integrated into a glass adaptor plate body through techniques like glass reflow, with low-resistance silicon or copper serving as the interconnect material. Optical sensors or laser diodes can be packaged by bonding the glass cover plate and adapter plate. This modular design has sizable industrial potential and can be utilized in various applications.

3.5. Thermoelectric Sensors

Based on the adjustable thermal conductivity, glass has attracted considerable attentions in the application of thermoelectric sensors. Thermoelectric sensors can convert temperature changes into electrical changes, allowing it to be applied to fabricate thermoelectric generators and wind sensors.

Thermoelectric Generators can transform temperature difference or low-grade waste heat into electricity. It has great application prospect in portable electronics, wireless sensors, medical devices. As glass boasts low thermal conductivity, it can effectively increase the temperature difference between hot and cold ends of micro thermocouples, enhancing the thermoelectric conversion capability, in combination with high aspect ratio TGVs. Liu et al[101] fabricated micro thermoelectric generators based on Bi2Te3 and Sb2Te3 using 200μm thick glass substrates. The vias were formed by laser ablation, and Bi2Te3 and Sb2Te3 were deposited in the vias at both ends of the device. The 200μm thick glass is capable of generating a temperature difference of 138K, which in turn provides an output voltage of 40.89mV and an output power of 19.72μW. Compared to photoresist masks, thermal sensors produced on glass substrates offer technical and cost benefits by allowing for more flexible control of the device's output voltage and power. Wind sensors are commonly used in areas such as agricultural production, transportation and energy harvesting. The wind force can be estimated by detecting subtle temperature changes on sensors caused by the wind. Miniaturized hot air sensors offer high initial sensitivity and low processing costs, but their reliance on heating for measurement results in high energy consumption. Glass is a low thermal conductivity material that can effectively reduce heat loss. Relying on TGV technology allows for electrical connections without the need for external wiring, meeting the requirements of reliability and high performance. Zhu et al [102-105] proposed a thermal wind sensor packaging scheme implemented using glass reflow technology. Drawing upon the performance benefits of the glass substrate and TGVs, the total heating power consumption of the sensor amounts to a mere 14.5mW.

4. Discussion

Wafer-level packaging offers considerable benefits for sensor packaging, and the TGV process is capable of achieving interconnection and bonding while maintaining reliability and process compatibility[25]. TGVs also allows for greater flexibility in establishing power supply and signal transmission rules, including the seamless integration of optical interconnections, capacitors, inductors, and other devices. Intel asserted that TGV technology will redefine chip packaging boundaries, offering transformative solutions for data centers, artificial intelligence, and graphics construction; propelling Moore's Law's advancements.

There are several methods of drilling glass, including mechanical techniques, wet etching, and laser methods. Mechanical drilling is considered the most straightforward form of processing. This method is also economical, making it an ideal choice for processing micro holes with low aspect ratios (1:1). By using fine drill bits and low-speed abrasives, high aspect ratios (e.g. 5:1) and producing fine holes (<100μm) can be achieved. The vias' inner wall is rough (around 1.6μm), and it takes on a conical shape when processed mechanically. The hole forming effect can be optimized through the addition of ultrasound or utilizing a mix of other methods.

The electrochemical machining method employs chemical etching along with the focused discharge method, resulting in higher machining efficiency (50μm/s) in comparison to mechanical machining. It is commonly used for machining vias with a thickness exceeding 300μm and a diameter greater than 280 μm, with aspect ratios ranging from 1:1 to 5:1. The vias created through the ECDM method are conical, and diameters are closely tied to the electrode being processed. Discharge-

 doi:10.20944/preprints202312.0064.v1

generated heat leads to thermal damage to the vias and splashing of melted glass. Optimizing the process may be possible by incorporating magnetic stirring in various ways.

Laser ablation, laser induced deep etching and photosensitive glass techniques have the potential to produce vias arrays with ultra-high aspect ratio (>10:1) and smaller size (<100μm), rendering them more fitting for wafer level packaging. The production capacity of the laser ablation method is dependent on the type of laser used. There are issues related to thermal stress and stress waves in vias. The heat affected region and debris resulting from laser ablation can be mitigated by the application of a protective surface layer or liquid processing. The processing technique of photosensitive glass is intricate, and the cost of the glass is high. However, it can achieve processing of various microstructures and any size of holes and grooves, and has high process compatibility. LIDE process is highly suitable for high aspect ratios TGVs processing and has a wide range of commercial applications. The current development direction of LIDE is the processing of TGVs with smaller diameters, higher aspect ratios, and wider ranges of glasses.

The glass reflux technique is often used to process motion sensors or MEMS devices such as accelerometers and gyroscopes. It enables the production of packaging substrates that meet the requirements of vertical interconnection, isolation protection and bonding. While the molten glass exhibits excellent filling ability, the capillary structure poses a challenge due to issues arising from surface tension. The process flow for the glass reflux method typically comprises anodic bonding, annealing, and double-sided thinning. The substrate requires a high level of surface cleanliness, and the processing is relatively intricate. Optimization methods, such as replacing glass substrates with glass powder, can reduce the process flow and save costs.

The TGV metallization process resembles the TSV metallization process but is simplified as it does not require a deposition barrier layer. The paste filling technique is appropriate for filling ultra-high verticality vias (>10:1) with low electrical performance demands. The paste filling method displays inferior stability, sealing, and process compatibility compared to the electroplating method. However, it is a cost-effective solution and provides excellent adhesion to glass. In contrast, electroplating demands good via morphology and roughness, and presents challenges in filling high aspect ratio through-holes. Blind holes facilitate seed layer filling, allowing electroplating filling and back thinning to produce vertical interconnection. The TGV created by electroplating generally employs copper as a conductor with minimal interconnect resistance, rendering it a good fit for applications that require high-frequency, high-speed, and three-dimensional packaging. The magnetic assembly method boasts a low process cost that permits the attainment of low-resistance and low-stress vertical interconnection. Nevertheless, regulating the magnetic force of conductive wires poses a challenge. Vias of different types and diameters require multiple magnets to achieve internal fixation. In addition, the process reliability of repeatedly filling the SOG is not high.

Glass substrates, such as BF33 and D263T borosilicate glass, are predominantly used in sensor packaging for both sealing and interconnecting purposes. These substrates possess excellent bonding performance and can be interconnected using TGV technology. Photoelectric and thermoelectric sensors can utilize the glass substrate's high transparency and low thermal conductivity to enhance device performance, while motion and pressure sensors can leverage the substrate's mechanical properties and sealing capability for greater device reliability. The outstanding dielectric and loss properties of glass can significantly reduce transmission loss, thereby expanding the range of sensor applications in the high-frequency and high-speed domains[106]. However, sensor packaging does not typically require high interconnection density or high aspect ratio interconnections at present, and there are few high-frequency and low-loss transmission applications. Therefore, mechanical drilling, chemical processing can be used to process vias, and electrical interconnection can be achieved by paste filling, evaporation plating, or conformal electroplating. The bonding and sealing performance notably affects device reliability and efficiency. Therefore, many MEMS sensors utilize glass reflow technology to fulfill the need for vertical interconnection and bonding, negating the need for extra electroplating and metallization procedures.

5. Conclusions

The article reviews the TGV process and sensor packaging applications. The TGV process comprises a glass through-hole manufacturing process and metallization process, and commonly used processing technologies are presented. The presented techniques for producing glass through-holes include abrasive spray processing, electrochemical discharge processing, laser ablation, photosensitive glass and glass reflow processing. The TGV metallization techniques introduced are conductive adhesive filling method, electroplating method and magnetic assembly method. We present packaging applications of TGV technology separately by sensor type and describe the TGV process flow and capabilities in detail. This article helps to select the appropriate TGV process according to the processing requirements of the sensor. TGV technology can be employed for the future development of sensor packaging towards smaller sizes, higher densities, and higher degrees of reliability in 3D integration, exhibiting promising potential for application.

Acknowledgment: This work is supported by the National Natural Science Foundation of China (Grant No. U2241222).

References

1. Yang, F.; Han, G.; Yang, J.; Zhang, M.; Ning, J.; Yang, F.; Si, C. Research on Wafer-Level MEMS Packaging with Through-Glass Vias. *Micromachines (Basel)* **2018**, *10*, doi:10.3390/mi10010015.
2. Kuang, Y.B.; Hou, Z.Q.; Zhuo, M.; Xu, Q.; Li, Q.S.; Xiao, B.; Shan, H.; Xiao, D.B.; Wu, X.Z.; Ieee. RESEARCH OF WAFER-LEVEL VACUUM PACKAGING BASED ON TGV TECHNOLOGY FOR MEMS DEVICES. In Proceedings of the 33rd IEEE International Conference on Micro Electro Mechanical Systems (MEMS), Vancouver, CANADA, Jan 18-22, 2020; pp. 988-991.
3. Adelegan, O.J.; Coutant, Z.A.; Zhang, X.; Yamaner, F.Y.; Oralkan, O.; Ieee. A 2D Capacitive Micromachined Ultrasonic Transducer (CMUT) Array with Through-Glass-Via Interconnects Fabricated Using Sacrificial Etching Process. In Proceedings of the IEEE International Ultrasonics Symposium (IUS), Glasgow, ENGLAND, Oct 06-09, 2019; pp. 1205-1208.
4. Stenchly, V.; Reinert, W.; Quenzer, H.J.; Iop. Modular packaging concept for MEMS and MOEMS. In Proceedings of the 28th Micromechanics and Microsystems Europe Workshop (MME), Uppsala, SWEDEN, Aug 23-25, 2017.
5. Ma, S.L.; Ren, K.L.; Xia, Y.M.; Yan, J.; Luo, R.F.; Cai, H.; Jin, Y.F.; Ma, M.J.; Jin, Z.H.; Chen, J. Process Development of a New TGV Interposer for Wafer Level Package of Inertial MEMS Device. In Proceedings of the 17th International Conference on Electronic Packaging Technology (ICEPT), Chinese Inst Elect, Elect Mfg & Packaging Technol Soc, Wuhan, PEOPLES R CHINA, Aug 16-19, 2016; pp. 983-987.
6. Wang, Y.X.; Ma, S.L.; Liu, X.Q.; Zhao, J.H.; Ieee. Partially filled TGV based on Double Sides Cu Conformal Electroplating Process for MEMS Vacuum Packaging. In Proceedings of the International Conference on Electronics Packaging (ICEP), Sapporo, JAPAN, May 11-14, 2022; pp. 53-54.
7. Fu, Y.C.; Han, G.W.; Gu, J.B.; Zhao, Y.M.; Ning, J.; Wei, Z.Y.; Yang, F.H.; Si, C.W. A High-Performance MEMS Accelerometer with an Improved TGV Process of Low Cost. *Micromachines* **2022**, *13*, doi:10.3390/mi13071071.
8. Yang, Z.; Wang, Y.; Wang, H.; Wang, Y.; Dai, X.; Ding, G.; Zhao, X.; Ieee. HIGH-G MEMS SHOCK THRESHOLD SENSOR INTEGRATED ON A COPPER FILLING THROUGH-GLASS-VIA (TGV) SUBSTRATE FOR SURFACE MOUNT APPLICATION. In Proceedings of the 18th International Conference on Solid-State Sensors, Actuators and Microsystems (TRANSDUCERS), Anchorage, AK, Jun 21-25, 2015; pp. 291-294.
9. Zhang, M.; Yang, J.; He, Y.R.; Yang, F.; Yang, F.H.; Han, G.W.; Si, C.W.; Ning, J. Research on a 3D Encapsulation Technique for Capacitive MEMS Sensors Based on Through Silicon Via. *Sensors* **2019**, *19*, doi:10.3390/s19010093.
10. Kuang, Y.B.; Xiao, D.B.; Zhou, J.; Li, W.Y.; Hou, Z.Q.; Cui, H.J.; Wu, X.Z. Theoretical model of glass reflow process for through glass via (TGV) wafer fabrication. *Journal of Micromechanics and Microengineering* **2018**, *28*, doi:10.1088/1361-6439/aac405.
11. Kuang, Y.B.; Xiao, D.B.; Zhou, J.; Zhuo, M.; Li, W.Y.; Hou, Z.Q.; Cui, H.J.; Wu, X.Z. Enhancing airtightness of TGV through regulating interface energy for wafer-level vacuum packaging. *Microsystem Technologies-*

Micro-and Nanosystems-Information Storage and Processing Systems **2018**, *24*, 3645-3649, doi:10.1007/s00542-018-3804-7.

12. Nguyen, T.; Pang, K.; Wang, J. A Preliminary Study of the Erosion Process in Micro-machining of Glasses with a Low Pressure Slurry Jet. In Proceedings of the 11th International Symposium on Advances in Abrasive Technology, Awaji City, JAPAN, 2009 Sep 30-Oct 03, 2008; pp. 375-380.
13. Qiu, Y.F.; Wang, C.Y.; Wang, J.; Song, Y.X. Masked and Unmasked Machining of Glass by Micro Abrasive Jet. In Proceedings of the 8th China-Japan International Conference on Ultra-Precision Machining, Changsha, PEOPLES R CHINA, Nov 24-25, 2008; pp. 182-+.
14. Fan, J.M.; Wang, J. Micro-channel fabrication on quartz crystals by a micro abrasive air jet. In Proceedings of the 3rd International Conference on Advances in Materials Manufacturing (ICAMMP 2012), Beihai, PEOPLES R CHINA, Dec 22-23, 2012; pp. 2159-2163.
15. Fan, J.M.; Wang, J. Kerf profile characteristics in abrasive air jet micromachining. In Proceedings of the 16th International Symposium on Advances in Abrasive Technology (ISAAT 2013), Hangzhou, PEOPLES R CHINA, Sep 23-26, 2013; pp. 33-38.
16. Nouraei, H.; Wodoslawsky, A.; Papini, M.; Spelt, J.K. Characteristics of abrasive slurry jet micro-machining: A comparison with abrasive air jet micro-machining. *Journal of Materials Processing Technology* **2013**, *213*, 1711-1724, doi:10.1016/j.jmatprotec.2013.03.024.
17. Kowsari, K.; Nouraei, H.; James, D.F.; Spelt, J.K.; Papini, M. Abrasive slurry jet micro-machining of holes in brittle and ductile materials. *Journal of Materials Processing Technology* **2014**, *214*, 1909-1920, doi:10.1016/j.jmatprotec.2014.04.008.
18. Nouraei, H.; Kowsari, K.; Spelt, J.K.; Papini, M. Surface evolution models for abrasive slurry jet micro-machining of channels and holes in glass. *Wear* **2014**, *309*, 65-73, doi:10.1016/j.wear.2013.11.003.
19. Nouhi, A.; Lari, M.R.S.; Spelt, J.K.; Papini, M. Implementation of a shadow mask for direct writing in abrasive jet micro-machining. *Journal of Materials Processing Technology* **2015**, *223*, 232-239, doi:10.1016/j.jmatprotec.2015.04.007.
20. Abhishek, K.; Hiremath, S.S. Machining of Micro-holes on Sodalime Glass using Developed Micro-Abrasive Jet Machine (μ-AJM). In Proceedings of the 1st Global Colloquium on Recent Advancements and Effectual Researches in Engineering, Science and Technology (RAEREST), St Josephs Coll Engn & Technol, Palai, INDIA, Apr 22-23, 2016; pp. 1234-1241.
21. Kowsari, K.; Schwartzentruber, J.; Spelt, J.K.; Papini, M. Erosive smoothing of abrasive slurry-jet micro-machined channels in glass, PMMA, and sintered ceramics: Experiments and roughness model. *Precision Engineering-Journal of the International Societies for Precision Engineering and Nanotechnology* **2017**, *49*, 332-343, doi:10.1016/j.precisioneng.2017.03.003.
22. Hou, R.G.; Wang, T.; Lv, Z.; Liu, Y.Y. Experimental Study of the Ultrasonic Vibration-Assisted Abrasive Waterjet Micromachining the Quartz Glass. *Advances in Materials Science and Engineering* **2018**, *2018*, doi:10.1155/2018/8904234.
23. Li, H.Z.; Wang, J.; Kwok, N.; Nguyen, T.; Yeoh, G.H. A study of the micro-hole geometry evolution on glass by abrasive air-jet micromachining. *Journal of Manufacturing Processes* **2018**, *31*, 156-161, doi:10.1016/j.jmapro.2017.11.013.
24. Qi, H.; Qin, S.; Cheng, Z.; Teng, Q.; Hong, T.; Xie, Y. Towards understanding performance enhancing mechanism of micro-holes on K9 glasses using ultrasonic vibration-assisted abrasive slurry jet. *Journal of Manufacturing Processes* **2021**, *64*, 585-593, doi:10.1016/j.jmapro.2021.01.048.
25. Hof, L.; Abou Ziki, J. Micro-Hole Drilling on Glass Substrates—A Review. *Micromachines* **2017**, *8*, doi:10.3390/mi8020053.
26. Takahashi, S.; Horiuchi, K.; Tatsukoshi, K.; Ono, M.; Imajo, N.; Mobely, T.; Ieee. Development of Through Glass Via (TGV) Formation Technology Using Electrical Discharging for 2.5/3D Integrated Packaging. In Proceedings of the IEEE 63rd Electronic Components and Technology Conference (ECTC), Las Vegas, NV, May 28-31, 2013; pp. 348-352.
27. Ho, C.C.; Wu, D.S. Characteristics of the Arcing Plasma Formation Effect in Spark-Assisted Chemical Engraving of Glass, Based on Machine Vision. *Materials* **2018**, *11*, doi:10.3390/ma11040470.
28. Ranganayakulu, J.; Srihari, P.V. Multi-objective Optimization Using Taguchi's Loss Function-Based Principal Component Analysis in Electrochemical Discharge Machining of Micro-channels on Borosilicate Glass with Direct and Hybrid Electrolytes. In Proceedings of the International Conference on Engineering Materials, Metallurgy and Manufacturing (ICEMMM, Chennai, INDIA, Feb 15-16, 2018; pp. 349-360.

29. Xu, Y.; Chen, J.H.; Jiang, B.Y.; Liu, Y.; Ni, J. Experimental investigation of magnetohydrodynamic effect in electrochemical discharge machining. *International Journal of Mechanical Sciences* **2018**, *142*, 86-96, doi:10.1016/j.ijmecsci.2018.04.020.
30. Arab, J.; Kannojia, H.K.; Dixit, P. Effect of tool electrode roughness on the geometric characteristics of through-holes formed by ECDM. *Precision Engineering-Journal of the International Societies for Precision Engineering and Nanotechnology* **2019**, *60*, 437-447, doi:10.1016/j.precisioneng.2019.09.008.
31. Kannojia, H.K.; Arab, J.; Pegu, B.J.; Dixit, P. Fabrication and Characterization of Through-Glass Vias by the ECDM Process. *Journal of the Electrochemical Society* **2019**, *166*, D531-D538, doi:10.1149/2.0141913jes.
32. Wuthrich, R.; Hof, L.A. Low Batch Size Production of Glass Products requiring Micrometer Precision. In Proceedings of the 13th International-Federation-of-Automatic-Control (IFAC) Workshop on Intelligent Manufacturing Systems (IMS), Oshawa, CANADA, Aug 12-14, 2019; pp. 319-322.
33. Kannojia, H.K.; Arab, J.; Sidhique, A.; Mishra, D.K.; Kumar, R.; Pednekar, J.; Dixit, P.; Ieee. Fabrication and Characterization of Through-glass vias (TGV) based 3D Spiral and Toroidal Inductors by Cost-effective ECDM Process. In Proceedings of the 70th IEEE Electronic Components and Technology Conference (ECTC), Electr Network, Jun 03-30, 2020; pp. 1192-1198.
34. Sahebari, S.M.S.; Barari, A.; Abou Ziki, J.D. Neural Network Signal Processing in Spark Assisted Chemical Engraving (SACE) Micromachining. In Proceedings of the 14th IEEE International Conference on Industry Applications (INDUSCON), Univ Sao Paulo, Escola Politecnica, ELECTR NETWORK, Aug 15-18, 2021; pp. 1169-1176.
35. Bajpai, V.K.; Mishra, D.K.; Dixit, P. Fabrication of Through-glass Vias (TGV) based 3D microstructures in glass substrate by a lithography-free process for MEMS applications. *Applied Surface Science* **2022**, *584*, doi:10.1016/j.apsusc.2022.152494.
36. Bahar, D.; Dvivedi, A.; Kumar, P. On innovative approach in ECDM process by controlling the temperature and stirring rate of the electrolyte. *Materials and Manufacturing Processes* **2023**, doi:10.1080/10426914.2023.2238057.
37. Villeneuve, G.; Hof, L.A. On the use of the current signal in spark assisted chemical engraving for micromachining process control. *Precision Engineering-Journal of the International Societies for Precision Engineering and Nanotechnology* **2023**, *83*, 181-191, doi:10.1016/j.precisioneng.2023.06.007.
38. Wu, Y.; Jia, W.; Wang, C.-Y.; Hu, M.; Ni, X.; Chai, L. Micro-hole fabricated inside FOTURAN glass using femtosecond laser writing and chemical etching. *Optical and Quantum Electronics* **2007**, *39*, 1223-1229, doi:10.1007/s11082-008-9192-y.
39. Zhang, J.; Li, Y.; Wang, W. Fabrication Technology of High Aspect Ratio Microholes Based on Photosensitive Glass. *Electronics Process Technology* **2022**, *43*, 139-142, doi:10.14176/j.issn.1001-3474.2022.03.005.
40. Freitag, A.; Vogel, D.; Scholz, R.; Dietrich, T.R. Microfluidic Devices Made of Glass. *JALA: Journal of the Association for Laboratory Automation* **2001**, *6*, 45-49, doi:10.1016/s1535-5535-04-00143-1.
41. Williams, J.D.; Schmidt, C.; Serkland, D. Processing advances in transparent Foturan^{A®} MEMS. *Applied Physics a-Materials Science & Processing* **2010**, *99*, 777-782, doi:10.1007/s00339-010-5721-1.
42. Mrotzek, S.; Harnisch, A.; Hülsenberg, D.; Brokmann, U. Crystallisation mechanism in ultraviolet sensitive microstructurable glasses. *Glass Technology* **2004**, *45*, 97-100.
43. Lin, L.; Wang, Q.; Qiu, D. Formation and Metallization Process Study on High Aspect Ratio Through-Glass-Via (TGV) Within Photosensitive Glass. *Transactions of Beijing Institute of Technology* **2018**, *38*, 52-57, doi:10.15918/j.tbit1001-0645.2018.01.009.
44. Brokmann, U.; Weigel, C.; Altendorf, L.-M.; Strehle, S.; Rädlein, E. Wet Chemical and Plasma Etching of Photosensitive Glass. *Solids* **2023**, *4*, 213-234.
45. Haque, R.-u.M.; Wise, K.D. A Glass-in-Silicon Reflow Process for Three-Dimensional Microsystems. *Journal of Microelectromechanical Systems* **2013**, *22*, 1470-1477, doi:10.1109/jmems.2013.2265851.
46. Toan, N.V.; Toda, M.; Ono, T. An Investigation of Processes for Glass Micromachining. *Micromachines* **2016**, *7*, doi:10.3390/mi7030051.
47. Luo, B.; Su, Z.X.; Shang, J.T.; Ieee. Glass Molding for Microstructures. In Proceedings of the 9th IEEE International Symposium on Inertial Sensors and Systems (IEEE INERTIAL), Avignon, FRANCE, May 08-11, 2022.
48. Du, X.; Liu, S.; Zhu, M. Reflow Technology of Nano-Glass Powder for TGV Packaging. *Micronanoelectronic Technology* **2020**, *57*, 562-567, doi:10.13250/j.cnki.wndz.2020.07.009.

49. Lee, S.K.; Kim, M.G.; Jo, K.W.; Shin, S.M.; Lee, J.H. A glass reflowed microlens array on a Si substrate with rectangular through-holes. *Journal of Optics a-Pure and Applied Optics* **2008**, *10*, doi:10.1088/1464-4258/10/4/044003.
50. Lin, C.-W.; Hsu, C.-P.; Yang, H.-A.; Wang, W.C.; Fang, W. Implementation of silicon-on-glass MEMS devices with embedded through-wafer silicon vias using the glass reflow process for wafer-level packaging and 3D chip integration. *Journal of Micromechanics and Microengineering* **2008**, *18*, doi:10.1088/0960-1317/18/2/025018.
51. Hu, Q.; Zhou, J.; Li, W. Modeling of glass-reflow facing TGV substrate. *Transducer and Microsystem Technologies* **2017**, *36*, 34-37, doi:10.13873/j.1000-9787(2017)09-0034-04.
52. Li, W.Y.; Xiao, D.B.; Wu, X.Z.; Hou, Z.Q.; Chen, Z.H.; Wang, X.H.; Zhou, J. A new fabrication process of TGV substrate with silicon vertical feedthroughs using double sided glass in silicon reflow process. *Journal of Materials Science-Materials in Electronics* **2017**, *28*, 3917-3923, doi:10.1007/s10854-016-6005-0.
53. Liu, Y.F.; Sang, H.B.; Bu, Z.X.; Zhang, Y.L.; Gao, G.G.; Wang, L.Y.; Ieee. Influence of the Particle Size of Glass Powder on Sintering Characteristics in TGV Packaging. In Proceedings of the 16th IEEE International Conference on Nano/Micro Engineered and Molecular Systems (IEEE-NEMS), Xiamen, PEOPLES R CHINA, Apr 25-29, 2021; pp. 1065-1068.
54. Nguyen Van, T.; Hahng, S.; Song, Y.; Ono, T. Fabrication of Vacuum-Sealed Capacitive Micromachined Ultrasonic Transducer Arrays Using Glass Reflow Process. *Micromachines* **2016**, *7*, doi:10.3390/mi7050076.
55. Chung, C.K.; Lin, S.L. CO₂ laser micromachined crackless through holes of Pyrex 7740 glass. *International Journal of Machine Tools & Manufacture* **2010**, *50*, 961-968, doi:10.1016/j.ijmachtools.2010.08.002.
56. Brusberg, L.; Queisser, M.; Gentsch, C.; Schröder, H.; Lang, K.D. Advances in CO₂-Laser Drilling of Glass Substrates. In Proceedings of the 7th Conference on Laser Assisted Net shape Engineering (LANE) / International Conference on Photonic Technologies, Furth, GERMANY, Nov 12-15, 2012; pp. 548-555.
57. Chung, C.K.; Lin, S.L.; Wang, H.Y.; Tan, T.K.; Tu, K.Z.; Lung, H.F. Fabrication and simulation of glass micromachining using CO₂ laser processing with PDMS protection. *Applied Physics a-Materials Science & Processing* **2013**, *113*, 501-507, doi:10.1007/s00339-013-7555-0.
58. Brusberg, L.; Queisser, M.; Neitz, M.; Schröder, H.; Lang, K.D.; Ieee. CO₂-Laser Drilling of TGVs for Glass Interposer Applications. In Proceedings of the IEEE 64th Electronic Components and Technology Conference (ECTC), Lake Buena Vista, FL, May 27-30, 2014; pp. 1759-1764.
59. Huang, H.; Yang, L.M.; Liu, J. Micro-hole drilling and cutting using femtosecond fiber laser. *Optical Engineering* **2014**, *53*, doi:10.1117/1.Oe.53.5.051513.
60. Sakakura, M.; Shimotsuma, Y.; Miura, K. Observation of Stress Wave and Thermal Stress in Ultrashort Pulse Laser Bulk Processing inside Glass. *Journal of Laser Micro Nanoengineering* **2017**, *12*, 159-164, doi:10.2961/jlmn.2017.02.0019.
61. Ito, Y.; Shinomoto, R.; Nagato, K.; Otsu, A.; Tatsukoshi, K.; Fukasawa, Y.; Kizaki, T.; Sugita, N.; Mitsuishi, M. Mechanisms of damage formation in glass in the process of femtosecond laser drilling. *Applied Physics a-Materials Science & Processing* **2018**, *124*, doi:10.1007/s00339-018-1607-4.
62. Sato, Y.; Imajyo, N.; Ishikawa, K.; Tummala, R.; Hori, M. Laser-drilling formation of through-glass-via (TGV) on polymer-laminated glass. *Journal of Materials Science-Materials in Electronics* **2019**, *30*, 10183-10190, doi:10.1007/s10854-019-01354-5.
63. Wlodarczyk, K.L.; Hand, D.P.; Maroto-Valer, M. Maskless, rapid manufacturing of glass microfluidic devices using a picosecond pulsed laser. *Scientific Reports* **2019**, *9*, doi:10.1038/s41598-019-56711-5.
64. Kondratenko, V.S.; Kadomkin, V.V.; Lu, H.T.; Naumov, A.S.; Velikovskii, I.E. Laser Drilling of Microholes in Glass. *Glass and Ceramics* **2020**, *77*, 39-42, doi:10.1007/s10717-020-00233-4.
65. Schrauben, J.N.; Matsumoto, H.; Lin, Z.B.; Kleinert, J. Rapid and complex dynamics of through glass via formation using a picosecond quasi-continuous wave laser as revealed by time-resolved absorptance measurements and multiphase modeling. *Applied Physics a-Materials Science & Processing* **2023**, *129*, doi:10.1007/s00339-023-06526-z.
66. Matsumoto, H.; Lin, Z.B.; Schrauben, J.N.; Kleinert, J.; Vázquez, R.G.; Buttazzoni, M.; Otto, A. Rapid formation of high aspect ratio through holes in thin glass substrates using an engineered, QCW laser approach. *Applied Physics a-Materials Science & Processing* **2022**, *128*, doi:10.1007/s00339-022-05404-4.

67. Ostholt, R.; Ambrosius, N.; Krüger, R.A. High speed through glass via manufacturing technology for interposer. In Proceedings of the Proceedings of the 5th Electronics System-integration Technology Conference (ESTC), 16-18 Sept. 2014, 2014; pp. 1-3.
68. Chen, L.; Yu, D. Investigation of low-cost through glass vias formation on borosilicate glass by picosecond laser-induced selective etching. *Journal of Materials Science-Materials in Electronics* **2021**, *32*, 16481-16493, doi:10.1007/s10854-021-06205-w.
69. Delrue, J.-P.; Ostholt, R.; Ambrosius, N.; Ieee. Glass Wafer Level Packaging Enabled by Laser Induced Deep Etching of Closed Cavities. In Proceedings of the 22nd European Microelectronics and Packaging Conference and Exhibition (EMPC), Pisa, ITALY, 2019 Sep 16-19, 2019.
70. Vanda, J.; Mydlar, M.; Pilna, K.; Turcicova, H.; Poboril, R.; Brajer, J.; Mocek, T.; Stoklasa, B.; Venos, S. LIDT testing as a tool for optimization of processing window for D263 glass sheet TGV treatment. In Proceedings of the 54th SPIE Laser Damage Symposium on Laser-Induced Damage in Optical Materials, Rochester, NY, 2022 Sep 18-21, 2022.
71. Beresna, M.; Gecevicius, M.; Kazansky, P.G. Polarization sensitive elements fabricated by femtosecond laser nanostructuring of glass Invited. *Optical Materials Express* **2011**, *1*, 783-795, doi:10.1364/ome.1.000783.
72. Rajesh, S.; Bellouard, Y.; Ieee. Towards fast femtosecond laser micromachining of glass, effect of deposited energy. In Proceedings of the Conference on Lasers and Electro-Optics (CLEO)/Quantum Electronics and Laser Science Conference (QELS), San Jose, CA, 2010 May 16-21, 2010.
73. Qi, J.; Wang, Z.; Xu, J.; Lin, Z.; Li, X.; Chu, W.; Cheng, Y. Femtosecond laser induced selective etching in fused silica: optimization of the inscription conditions with a high-repetition-rate laser source. *Optics Express* **2018**, *26*, 29669-29678, doi:10.1364/oe.26.029669.
74. Serkov, A.A.; Snelling, H.V. Enhanced chemical etch rate of borosilicate glass via spatially resolved laser-generated color centers. *Journal of Physics D-Applied Physics* **2020**, *53*, doi:10.1088/1361-6463/ab6515.
75. Available online: https://mp.weixin.qq.com/s/O0bQFmkf_RxvflcrwdKhQQ (accessed on
76. Chen, L.; Wu, H.; Zhang, M.C.; Jiang, F.; Yu, T.; Yu, D.Q.; Ieee. Development of Laser-Induced Deep Etching Process for Through Glass Via. In Proceedings of the 20th International Conference on Electronic Packaging Technology (ICEPT), Hong Kong, HONG KONG, Aug 12-15, 2019.
77. Laakso, M.J.; Bleiker, S.J.; Liljeholm, J.; Martensson, G.E.; Asiatici, M.; Fischer, A.C.; Stemme, G.; Ebefors, T.; Niklaus, F. Through-Glass Vias for Glass Interposers and MEMS Packaging Applications Fabricated Using Magnetic Assembly of Microscale Metal Wires. *IEEE Access* **2018**, *6*, 44306-44317, doi:10.1109/access.2018.2861886.
78. Wei, T.W.; Wang, Q.; Cai, J.; Chen, L.; Huang, J.; Wang, L.; Zhang, L.; Li, C.; Ieee. Performance and Reliability Study of TGV Interposer in 3D Integration. In Proceedings of the IEEE 16th Electronics Packaging Technology Conference (EPTC), Marina Bay Sands, SINGAPORE, Dec 03-05, 2014; pp. 601-605.
79. Kudo, H.; Akazawa, M.; Yamada, S.; Tanaka, M.; Iida, H.; Suzuki, J.; Takano, T.; Kuramochi, S.; Ieee, T.P.C. High-speed High-density Cost-effective Cu-filled Through-Glass-Via Channel for Heterogeneous Chip Integration. In Proceedings of the International Conference on Electronics Packaging (ICEP), Niigata, JAPAN, Apr 17-20, 2019; pp. 104-109.
80. Onohara, J.; Takagi, F.; Kizu, T.; Imayoshi, K.; Nomura, H.; Yun, H.B.; Ieee. Development of the Integrated Passive Device using Through-Glass-Via substrate. In Proceedings of the International Conference on Electronics Packaging (ICEP) / iMAPS All Asia Conference (IAAC), Kuwana, JAPAN, Apr 17-21, 2018; pp. 19-22.
81. Tanaka, M.; Kuramochi, S.; Tai, T.; Sato, Y.; Kidera, N.; Ieee. High Frequency Characteristics of Glass Interposer. In Proceedings of the 70th IEEE Electronic Components and Technology Conference (ECTC), Electr Network, Jun 03-30, 2020; pp. 601-610.
82. Kilige, S.; Bartusseck, I.; Junige, M.; Neumann, V.; Reif, J.; Wenzel, C.; Böttcher, M.; Albert, M.; Wolf, M.J.; Bartha, J.W. 3D system integration on 300 mm wafer level: High-aspect-ratio TSVs with ruthenium seed layer by thermal ALD and subsequent copper electroplating. *Microelectronic Engineering* **2019**, *205*, 20-25, doi:10.1016/j.mee.2018.11.006.
83. Van Huylenbroeck, S.; Li, Y.L.; Heylen, N.; Croes, K.; Beyer, G.; Beyne, E.; Brouri, M.; Gopinath, S.; Nalla, P.; Thorum, M.; et al. Advanced Metallization Scheme for 3x50µm Via Middle TSV and Beyond. In Proceedings of the IEEE 65th Electronic Components and Technology Conference (ECTC), San Diego, CA, May 26-29, 2015; pp. 66-72.

84. Vandersmissen, K.; Inou, F.; Velenis, D.; Li, Y.; Dictus, D.; Frees, B.; Van Huylenbroeck, S.; Kondo, M.; Seino, T.; Heylen, N.; et al. Demonstration of a cost effective Cu electroless TSV metallization scheme. In Proceedings of the 24th Workshop on Materials for Advanced Metallization held Jointly with the International Interconnect Technology (IITC) Conference, Grenoble, FRANCE, May 18-21, 2015; pp. 197-199.
85. Inoue, F.; Philipsen, H.; Radisic, A.; Armini, S.; Civale, Y.; Leunissen, P.; Kondo, M.; Webb, E.; Shingubara, S. Electroless Cu deposition on atomic layer deposited Ru as novel seed formation process in through-Si vias. *Electrochimica Acta* **2013**, *100*, 203-211, doi:10.1016/j.electacta.2013.03.106.
86. Inouel, F.; Philipsen, H.; van der Veen, M.H.; Van Huylenbroeck, S.; Armini, S.; Struyf, H.; Tanaka, T.; Ieee. Electroless Cu Seed on Ru and Co Liners in High Aspect Ratio TSV. In Proceedings of the IEEE International Interconnect Technology Conference / Advanced Metallization Conference (IITC/AMC), San Jose, CA, May 20-23, 2014; pp. 207-209.
87. Zhang, Z.Y.; Ding, Y.T.; Xiao, L.; Cai, Z.R.; Yang, B.Y.; Chen, Z.M.; Xie, H.K. Enabling Continuous Cu Seed Layer for Deep Through-Silicon-Vias With High Aspect Ratio by Sequential Sputtering and Electroless Plating. *Ieee Electron Device Letters* **2021**, *42*, 1520-1523, doi:10.1109/led.2021.3105667.
88. Lee, J.Y.; Lee, S.W.; Lee, S.K.; Park, J.H.; Ieee. WAFER LEVEL PACKAGING FOR RF MEMS DEVICES USING VOID FREE COPPER FILLED THROUGH GLASS VIA. In Proceedings of the 26th IEEE International Conference on Micro Electro Mechanical Systems (MEMS), Taipei, TAIWAN, Jan 20-24, 2013; pp. 773-776.
89. Tanaka, M.; Okazaki, Y.; Suyama, J.; Kuramochi, S.; Han, Y.G.; Horiuchi, O.; Katoh, Y.; Ieee. Experimental Study of Through Glass Via Effects on High Frequency Electrical Characteristics. In Proceedings of the International Conference on Electronics Packaging (ICEP) / iMAPS All Asia Conference (IAAC), Kuwana, JAPAN, Apr 17-21, 2018; pp. 184-188.
90. Gu, J.B.; Xia, X.Y.; Zhang, W.B.; Li, X.X.; Ieee. A Modified MEMS-Casting Based TSV Filling Method with Universal Nozzle Piece That Uses Surface Trenches as Nozzles. In Proceedings of the 19th International Conference on Electronic Packaging Technology (ICEPT), Inst Microelectron Chinese Acad Sci, Shanghai, PEOPLES R CHINA, Aug 08-11, 2018; pp. 536-539.
91. Kim, J.-K.; Baek, C.-W. Capacitive pressure sensor with wafer-through silicon vias using SOI-Si direct wafer bonding and glass reflow technique. *Ieice Electronics Express* **2013**, *10*, doi:10.1587/elex.10.20130453.
92. Luo, Z.; Chen, D.; Wang, J.; Li, Y.; Chen, J. A High-Q Resonant Pressure Microsensor with Through-Glass Electrical Interconnections Based on Wafer-Level MEMS Vacuum Packaging. *Sensors* **2014**, *14*, 24244-24257, doi:10.3390/s141224244.
93. Herickhoff, C.D.; van Schaijk, R. cMUT technology developments. *Zeitschrift Fur Medizinische Physik* **2023**, *33*, 256-266, doi:10.1016/j.zemedi.2023.04.010.
94. Zhang, X.; Yamaner, F.Y.; Oralkan, O.; Ieee. Fabrication of Capacitive Micromachined Ultrasonic Transducers with Through-Glass-Via Interconnects. In Proceedings of the IEEE International Ultrasonics Symposium (IUS), Taipei, TAIWAN, Oct 21-24, 2015.
95. Zhang, X.; Yamaner, F.Y.; Oralkan, Ö.; Ieee. Fabrication of Capacitive Micromachined Ultrasonic Transducers with Through-Glass-Via Interconnects. In Proceedings of the IEEE International Ultrasonics Symposium (IUS), Taipei, TAIWAN, Oct 21-24, 2015.
96. Adelegan, O.J.; Coutant, Z.A.; Zhang, X.; Yamaner, F.Y.; Oralkan, Ö.; Ieee. A 2D Capacitive Micromachined Ultrasonic Transducer (CMUT) Array with Through-Glass-Via Interconnects Fabricated Using Sacrificial Etching Process. In Proceedings of the IEEE International Ultrasonics Symposium (IUS), Glasgow, ENGLAND, Oct 06-09, 2019; pp. 1205-1208.
97. Adelegan, O.J.; Coutant, Z.A.; Zhang, X.; Yamaner, F.Y.; Oralkan, O. Fabrication of 2D Capacitive Micromachined Ultrasonic Transducer (CMUT) Arrays on Insulating Substrates With Through-Wafer Interconnects Using Sacrificial Release Process. *Journal of Microelectromechanical Systems* **2020**, *29*, 553-561, doi:10.1109/jmems.2020.2990069.
98. Chen, Z.H.; Yu, D.Q.; Jiang, F. Development of 3-D Wafer Level Packaging for SAW Filters Using Thin Glass Capping Technology. *Ieee Transactions on Components Packaging and Manufacturing Technology* **2022**, *12*, 375-381, doi:10.1109/tcpmt.2022.3140863.
99. Brusberg, L.; Schröder, H.; Töpper, M.; Arndt-Staufenbiel, N.; Röder, J.; Lutz, M.; Reichl, H.; Ieee. Thin Glass Based Packaging Technologies for Optoelectronic Modules. In Proceedings of the 59th Electronic Components and Technology Conference, San Diego, CA, May 26-29, 2009; pp. 207-212.

100. Brusberg, L.; Schröder, H.; Töpper, M.; Reichl, H.; Ieee. Photonic System-in-Package Technologies Using Thin Glass Substrates. In Proceedings of the 11th Electronics Packaging Technology Conference, Shangri La, SINGAPORE, Dec 09-11, 2009; pp. 930-+.
101. Liu, S.; Hu, B.; Liu, D.; Li, F.; Li, J.-F.; Li, B.; Li, L.; Lin, Y.-H.; Nan, C.-W. Micro-thermoelectric generators based on through glass pillars with high output voltage enabled by large temperature difference. *Applied Energy* **2018**, *225*, 600-610, doi:10.1016/j.apenergy.2018.05.056.
102. Zhu, Y.Q.; Chen, B.; Qin, M.; Huang, J.Q.; Huang, Q.A.; Ieee. A Self-packaged Self-heated Thermal Wind Sensor With High Reliability and Low Power Consumption. In Proceedings of the IEEE 10th International Conference on Nano/Micro Engineered and Molecular Systems (NEMS), Xian, PEOPLES R CHINA, Apr 07-11, 2015; pp. 193-196.
103. Zhu, Y.Q.; Chen, B.; Qin, M.; Huang, Q.A.; Huang, J.Q.; Ieee. Development of A Robust 2-D Thermal Wind Sensor Using Glass Reflow Process For Low Power Applications. In Proceedings of the IEEE 65th Electronic Components and Technology Conference (ECTC), San Diego, CA, May 26-29, 2015; pp. 1633-1639.
104. Zhu, Y.Q.; Chen, B.; Gao, D.; Qin, M.; Huang, Q.A.; Huang, J.Q. A robust and low-power 2-D thermal wind sensor based on a glass-in-silicon reflow process. *Microsystem Technologies-Micro-and Nanosystems-Information Storage and Processing Systems* **2016**, *22*, 151-162, doi:10.1007/s00542-015-2423-9.
105. Zhu, Y.Q.; Qin, M.; Ye, Y.Z.; Yi, Z.X.; Long, K.W.; Huang, Q.A. Modelling and characterization of a robust, low-power and wide-range thermal wind sensor. *Microsystem Technologies-Micro-and Nanosystems-Information Storage and Processing Systems* **2017**, *23*, 5571-5585, doi:10.1007/s00542-017-3361-5.
106. Watanabe, A.O.; Lin, T.H.; Ali, M.; Ogawa, T.; Raj, P.M.; Tentzeris, M.M.; Tummala, R.R.; Swaminathan, M.; Ieee. 3D Glass-Based Panel-Level Package with Antenna and Low-Loss Interconnects for Millimeter-Wave 5G Applications. In Proceedings of the IEEE MTT-S International Microwave Conference on Hardware and Systems for 5G and Beyond (IMC-5G), Atlanta, GA, Aug 15-16, 2019.